Food Science and Human Wellness
*食品科学与人类健康(英文)*
ISSN 2213-4530,CN 10-1750/TS

# 《Food Science and Human Wellness》网络首发论文

题目： In vitro anti-photoaging activity of fermented polysaccharides from Sargassum fusiforme by Lactobacillus plantarum

作者： Zetong Sun，Ting Duan，Biyang Zhu，Oliy Akhmedov，Lijun You

收稿日期： 2025-06-25
网络首发日期： 2025-08-29
引用格式： Zetong Sun，Ting Duan，Biyang Zhu，Oliy Akhmedov，Lijun You．In vitro anti-photoaging activity of fermented polysaccharides from Sargassum fusiforme by Lactobacillus plantarum[J/OL]．Food Science and Human Wellness.
https://link.cnki.net/urlid/10.1750.TS.20250829.1504.006

DOI: 10.26599/FSHW.2025.9250712



Contents lists available at CNKI

Food Science and Human Wellness

journal homepage: http://www.keaipublishing.com/en/journals/food-science-and-human-wellness

# *In vitro* anti-photoaging activity of fermented polysaccharides from *Sargassum fusiforme* by *Lactobacillus plantarum*

Zetong Sun[a], Ting Duan[a], Biyang Zhu[b], Oliy Akhmedov[c], Lijun You[a d]*

[a] *School of Food Science and Engineering, South China University of Technology, Guangzhou, 510640, China*

[b] *College of Light Industry and Food Engineering, Guangxi University, Nanning, 530004, China*

[c] *Institute of Bioorganic Chemistry of the Academy of Sciences of Uzbekistan, 83 M. Ulugbek str., 100125 Tashkent, Uzbekistan*

[d] *Research Institute for Food Nutrition and Human Health (111 Center), Guangzhou, Guangdong, China*

**ABSTRACT:** High molecular weights of seaweed polysaccharides usually limit their bioavailability. Fermentation of polysaccharides can reduce their molecular weight and improve their bioactivity, which effectively increase their application in food industry. In this study, *Lactobacillus plantarum* was used to ferment *Sargassum fusiforme* polysaccharides (SFP). The structure of fermented polysaccharide was characterized. Results showed that fermentation drastically reduced the average molecular weight of SFP by 75.2%. The percentage of reducing sugars and uronic acid gradually increased with time during fermentation. The functional groups of the fermented polysaccharides did not change, but the apparent morphology changed from rough and porous to smooth and fragmented. Fermented SFP exhibited better anti-photoaging activity in UVB-irradiated HaCaT cells. Specifically, it increased cell viability and hydroxyproline level. Additionally, it promoted the gene expression of Pro-collagen I α1 synthesis while inhibiting matrix metalloproteinases (MMP-1, MMP-3, MMP-9) and pro-inflammatory cytokines (IL-1β, TNF-α). These findings suggested that fermentation could enhance the anti-photoaging activity of seaweed polysaccharide, and could be developed as an alternative method for degrading polysaccharides.

**Keywords:** Anti-photoaging activity; *Lactobacillus plantarum*; fermentation; polysaccharides; HaCaT cell

## 1. Introduction

Skin photoaging, primarily induced by ultraviolet (UV) radiation, has become a significant dermatological concern due to increasing environmental stressors and lifestyle changes. UV exposure triggers the overproduction of reactive oxygen species (ROS), leading to collagen degradation and impaired skin barrier function [1]. Effective strategies to mitigate these effects are urgently needed. Marine resources, particularly seaweeds, are rich sources of bioactive compounds, of which polysaccharides are one of the most extensively studied [2]. Seaweed polysaccharides exhibit diverse biological activities, including anti-inflammatory [3, 4], anti-tumor [5-7], and immunomodulatory activity [8-12]. Notably, their potential in combating skin photoaging has attracted growing interest [13, 14].

***Corresponding author**
feyoulijun@scut.edu.cn

Received 25 June 2025
Received in revised from 26 July 2025
Accepted 4 August 2025

Sargassum fusiforme (SF) is a species of brown alga that belongs to the Sargassum genus. It is found in China, Japan, and South Korea. Its main components are alginic acid, fucoidan and laminaran[15]. Polysaccharides account for 20%-70% of SF's dry weight and are one of its most important bioactive components. Research has shown that SF polysaccharides exhibit various pharmacological activities, including antioxidant and anti-ageing properties, as well as the ability to enhance the immune system. SF polysaccharides also demonstrate potential in the prevention and treatment of cancer, helping to regulate the immune system and acting as hypoglycaemic and hypolipidaemic agents to aid in the management of diabetes and its complications[16]. However, the practical application of seaweed polysaccharides is greatly limited by its high molecular weight and low bioavailability [17].

There are many ways to process polysaccharides, such as acid hydrolysis, enzymatic hydrolysis, and ultrasonic-assisted degradation. However, acid hydrolysis requires high temperature and strong acid, as well as the problem of easy detachment of sulfate sites, which can affect the activity of polysaccharides[18]. Enzyme hydrolysis also faces problems. Firstly, enzymes are prone to deactivation and have high specificity, and pH and temperature optimization are required during the experimental process, greatly increasing the application cost[19]. Secondly, ultrasound assisted extraction of polysaccharides requires high instrument conditions and costs, making it difficult to apply on a large scale. And the degree of structural damage is high, making it prone to sugar chain breakage[20]. In this study, to address these limitations, we adopted fermentation technology as a powerful strategy for degrading polysaccharides. Because this process utilizes microbial metabolism to degrade and transform polysaccharides under mild conditions, avoiding the need for harsh chemical treatments or high energy consumption [21]. Recent studies have shown that fermentation reduces the molecular weight of polysaccharides. The molecular weight of yam polysaccharides fermented by *Saccharomyces cerevisiae* was significantly reduced by 6.1 times. Meanwhile, the metabolites during fermentation enhanced their antioxidant capacity [22]. Microbial enzymes produced during fermentation selectively cleave polysaccharide chains, result in low molecular weight fragments with improved bioactivity [23, 24]. Therefore, fermentation is a highly efficient and environmentally friendly way to enhance the functionality of seaweed polysaccharide. However, the changes in structural and bioactivity during fermentation remain unclear.

In this study, *Lactobacillus plantarum* was employed to ferment *Sargassum fusiforme* polysaccharides (SFP), the changes in the structure and anti-photoaging activity during fermentation were studied. Our findings will provide a promising approach to improve the solubility and bioactivity of polysaccharides.

## 2. Materials and methods

### *2.1 Materials and chemicals*

*Sargassum fusiforme* was collected in March 2024 from the coastal region of Wenzhou, Zhejiang Province, China. The harvested seaweed samples were meticulously rinsed with distilled water to remove impurities, followed by sun-drying to reduce moisture content. The dried samples were then ground into a fine powder using a commercial grinder (Model FW135, Tianjin Taisite Instrument Co., Ltd., Tianjin, China) and

sieved through a 40-mesh standard sieve to ensure uniform particle size. Ultra-micro powder production for subsequent analysis was achieved through micronization of the powder using the XDW-6BI ultra-micro pulverizer (Jinan Tatsu Micro Machinery Co. Ltd., Jinan, Shandong Province, China). The raw materials used in this study were mixed samples from a single batch, which was harvested from the same plot of land during the same harvest period. Subsequent experiments were conducted using samples of this mixed powder to ensure consistent growing, harvesting, storage, and transportation conditions.

Dextran standards with average molecular weights of 3.33, 4.66, 12.6, 63.3, 126, and 556 kDa, respectively. as well as monosaccharide standards (glucose, fucose, galactose, arabinose, xylose, fructose, galacturonic acid, and glucuronic acid), were procured from Sigma-Aldrich Chemical Co. (St. Louis, MO, USA). Cell culture reagents employed included Dulbecco's Modified Eagle's Medium (DMEM), fetal bovine serum (FBS), penicillin-streptomycin, phosphate-buffered saline (PBS), and trypsin-ethylenediaminetetraacetic acid (EDTA) solution, were purchased from Gibco Biotechnology Co., Ltd. (Grand Island, NY, USA). While gene primers were commercially synthesized at Sangon Biotech Co., Ltd. (Shanghai, China). All remaining chemicals were analytical-grade reagents.

*2.2 Strains and cultures*

*Lactobacillus plantarum* (LP) was extracted from traditional Chinese fermented foods. It was stored in Lactobacilli MRS Broth (MRS) containing glycerol (150 mL/L) at -80 ℃. The strain was firstly activated by dropping 100 μL of the culture into 2 mL of liquid MRS medium, and then transferred to a solid MRS colony counting plate and incubated at 37 ℃ for 24 h. The colonies were picked and inoculated into 2 mL of liquid MRS medium, and then continued to be incubated for 24 h. After that, the cells were collected by centrifugation (7000×g, 10 min, 4 ℃) (Centrifuge 5424R, Eppendorf, Guangzhou, China).

*2.3 Extraction and fermentation of polysaccharides from Sargassum fusiforme*

*Sargassum fusiforme* crude polysaccharide (named SFP) was prepared using our previously reported method [25]. Briefly, the obtained *Sargassum fusiforme* polysaccharides were lyophilized and dissolved and configured into three different concentration groups: 1%, 2% and 3% (w/v), respectively. Autoclave sterilization was performed at 105 ℃ for 15 min. After cooling at room temperature, 3.5 log CFU/mL of LP cell cultures were inoculated into the *Sargassum fusiforme* polysaccharide solution. Anaerobic fermentation was carried out at 37 ℃ for 1, 2 and 3 days. The supernatant was collected by centrifugation (7000 × g, 15 min, 4 ℃), and the supernatant was dialyzed through a 3 kDa dialysis bag for 48 h. The supernatant was collected by centrifugation (7000 × g, 15 min, 4 ℃). Finally, the dialysate was collected, evaporated and concentrated and lyophilized to obtain fermented *Sargassum fusiforme* polysaccharides (FSFPs). The polysaccharide sample fermented at 1% concentration group for 1 day was named FSFP-11, The polysaccharide sample fermented at 1% concentration group for 2 days was named FSFP-12. By such naming rules, The FSFPs were named FSFP-11 (1%, 1 day), FSFP-12 (1%, 2 days), FSFP-13 (1%, 3 days), FSFP-21 (2%, 1 day), FSFP-22 (2%, 2 days), FSFP-23 (2%, 3 days), FSFP-31 (3%, 1 day), FSFP-32 (3%, 2 days), and FSFP-33 (3%, 3 days), respectively. All fermentations were carried out independently in triplicate.

*2.4 The pH determination during fermentation*

The pH values of the *Sargassum fusiforme* polysaccharides samples were measured at 0, 12, 24, 36, 48, 60 and 72 hours of fermentation, respectively, using an FE28-Standard pH meter (Mettler Toledo, Shanghai, China). The pH changes were monitored to assess the acid production by *Lactobacillus plantarum* during fermentation.

*2.5 Colony-forming unit counting (CFU)*

Fermented polysaccharide solution was serially diluted with sterile saline to obtain proper concentration (*C1*). The number of bacterial colonies (*N1*) was measured by spot sampling on MRS solid medium plates, with three replicates for each dilution concentration. Three replicates were set up for each dilution, and the sample volume was 10 μL. Fermented stroke physiological saline solution (FSPSS) was set up as a control. Depending on the number of fermentation days, these FSPSS were named FSPSS-1, FSPSS-2 and FSPSS-3, respectively. Mean colony counts were expressed as a *log CFU/mL* formula calculation (1).

$$\log CFU/mL:\ \log\left(\frac{N1}{C1\times 0.01}\right) \quad (1)$$

*2.6 Chemical composition and structure of Sargassum fusiforme polysaccharides*

*2.6.1 Chemical composition*

The dinitrosalicylic acid (DNS) method quantified reducing sugar content, employing glucose calibration standards [26]. Carbazole-sulfuric acid colorimetry quantified glycuronic acid, with glucuronic acid serving as the calibration standard [27], glucuronic acid constitutes the predominant glycuronic acid in *Sargassum fusiforme* polysaccharides [28]. Barium sulfate turbidimetry quantified sulfate content, with potassium sulfate serving as the calibration standard [29]. The total phenol content was determined by the Folin-Ciocalteu assay using gallic acid as the standard [30]. Protein content was measured using the Bradford assay, standardized on bovine serum albumin [31].

*2.6.2 Average molecular weight*

Polysaccharide molecular weights were determined through HPGPC analysis, using a previous method with some modifications [32]. The HPGPC system (Shimadzu LC-20A, Shimadzu Instrument Co., Ltd., Tokyo, Japan) was equipped with two TSK-GEL columns connected in series: a G-3000PWXL column (7.8 mm × 300 mm, 7 μm) and a G-6000PWXL column (7.8 mm × 300 mm, 13 μm), both from Tosoh Corporation, Tokyo, Japan. The mobile phase was 0.02 M potassium dihydrogen phosphate ($KH_2PO_4$), delivered at a flow rate of 0.5 mL/min. A Waters 2414 refractive index detector (Waters Co. Ltd., Milford, MA, USA) facilitated detection at a column-oven maintained temperature of (35 ± 1) ℃. Prior to analysis, the polysaccharide samples were dissolved in 0.02 mol/L $KH_2PO_4$, filtered through a 0.22 μm membrane, and injected into the system at a volume of 25 μL. The calibration curve constructed from dextran standard (3.33, 4.66, 12.6, 63.3, 126, and 556 kDa, respectively) can calculate the average molecular weight of polysaccharides.

*2.6.3 Monosaccharide composition*

Ion chromatography (IC) was used for the determination of monosaccharide components in polysaccharides and the analytical method was as previously described with some modifications [33]. An ion chromatography system equipped with an electrochemical detector (Dionex ICS-3000, Dionex Corp., Sunnyvale, CA) was used for analysis, with a CarboPac chromatographic column ™ PA20 (3 mm ×150 mm), column temperature box maintains a constant temperature of 30 ℃. The mobile phase is a mixture of ultrapure water and NaOH solution (see supplementary materials for gradient program), with a constant flow rate of 0.5 mL/min. The sample was treated with acid hydrolysis, and 20 mg of polysaccharide sample was taken. A 2 mol/L trifluoroacetic acid solution was added and subjected to sealed hydrolysis at 105 ℃ for 6 hours. Then, the residue was dissolved in methanol and evaporated again under reduced pressure at 60 ℃ (repeated 5 times). After reconstitution with ultrapure water, it was filtered through a 0.22 μm microporous membrane. Inject 15 μL of sample solution into the chromatography system. Establish calibration curves based on monosaccharide standards (fucose, arabinose, galactose, glucose, xylose, galacturonic acid, glucuronic acid), and calculate the mole percentages of each monosaccharide through peak area integration.

*2.6.4 Scanning Electron Microscope (SEM) analysis*

The morphology and microstructure of polysaccharides were characterized by a scanning electron microscope (Merlin, Carl Zeiss AG, Oberkohen, Baden-Wurttemberg, Germany) to characterize the morphology and microstructure of polysaccharides. SEM structural analysis of lyophilized polysaccharides employed gold-sputtered specimens imaged at 100℃ under vacuum. The stage was observed under an acceleration voltage of 5 kV. The magnifications of the micrographs were 500 and 2000 times, respectively.

*2.6.5 Fourier Transform Infrared Spectrometer (FTIR) spectra analysis*

The samples were placed on the surface of an infrared ATR element and the infrared beam was passed through the ATR element to detect the polysaccharide functional groups. A FTIR spectrophotometer (Tensor27, Bruker GmbH, Bergisch Gladbach, Germany) was used to detect wavelengths in the range of 4000 $cm^{-1}$ to 500 $cm^{-1}$.

*2.7 2,2-Diphenyl-1-picrylhydrazyl (DPPH) radical activity assay*

The DPPH radical scavenging activity of polysaccharide was determined according to the method reported by Yamaguchi with some modifications [34]. The assay was conducted in a 96-well plate. The treatments applied were as follows: A1 (Control): 100 μL water + 100 μL DPPH radical solution (0.1 mmol/L in ethanol). A2 (Sample): 100 μL sample + 100 μL DPPH radical solution (0.1 mmol/L in ethanol). A3 (Blank): 100 μL sample + 100 μL anhydrous ethanol. Following a 30-minute incubation period, absorbance readings were taken at 517 nm. The results were used to calculate the DPPH scavenging activity by the equation (2).

$$Scavenging\ \ activity\ \ (\%):\ \left(1-\frac{A2-A3}{A1}\right)\times 100 \qquad (2)$$

### *2.8 Anti-photoaging activity of Sargassum fusiforme polysaccharides*

#### *2.8.1 Cell Culture and UVB Irradiation*

The human keratinocyte-forming cell line was obtained from the Cell Resource Center of Peking Union Medical College Hospital, Chinese Academy of Medical Sciences, and was transferred to 25 $cm^2$ culture flasks and cultured in DMEM containing 10% fetal bovine serum, 100 U/mL penicillin, and 100 μg/mL streptomycin in a humidified incubator at 37 ℃ with 5% $CO_2$, and the medium was changed three times a week. The method of UV irradiation was based on the method previously reported by our research group with a simple modification, 4 $mJ/cm^2$ UVB irradiation was applied to the cells [35].

#### *2.8.2 Cytotoxicity determination of polysaccharide samples*

The effect of SFP and FSFPs (FSFP-11, FSFP-12, FSFP-21, FSFP-22, FSFP-31, FSFP-32, respectively) on the viability of photoaged HaCaT cells were determined using the 3-(4,5-dimethylthiazol-2-yl)-2,5-diphenyltetrazolium bromide (MTT) assay. HaCaT cells were cultured for 24 h, rinsed with PBS, and then inoculated into 96-well plates at a ratio of $2 \times 10^4$ cells per well. After 24 h of incubation at 37 ℃, the medium was discarded, the cells were rinsed with PBS, and then cultured for 24 h in medium containing different concentrations of hyaluronic acid (positive control) (125, 250 and 500 μg/mL, respectively) and samples. After removal of the culture medium, cell viability was measured by MTT assay. Cell viability was detected by Cell Proliferation and Cytotoxicity Detection Kit (G020-1, Nanjing Jiancheng Bioengineering Institute, Nanjing, China).

#### *2.8.3 Determination of cell viability*

The cell viability experiments were performed in the same way as in section 2.8.2, except that after 24 h of sample medium incubation, the medium was discarded, the cells were rinsed with PBS, and the cells were subjected to 4 $mJ/cm^2$ of UVB radiation in a skin photo-aging apparatus (HOPE-MED 8101) (after UVB irradiation, cells were incubated with DMEM instead of PBS for 24 h at 37 ℃). After removing the culture medium, the cell viability was detected by MTT assay. Cell viability was detected by cell proliferation and cytotoxicity assay kit (G020-1, Nanjing Jiancheng Bioengineering Institute).

#### *2.8.4 Determination of hydroxyproline (HYP) Level*

HaCaT cells were seeded in 12-well plates at a concentration of $2.5 \times 10^5$ per well and treated as described in this section. Cell-free culture supernatants were collected and HYP levels were measured using the HYP Assay Kit (A030-1-1, Nanjing Jiancheng Bioengineering Institute, Nanjing, China). The positive control group was treated using hyaluronic acid (HA).

#### *2.8.5 Determination of MMP-1, MMP-3, MMP-9*

The levels of MMP-1, MMP-3, and MMP-9 were measured using MMP-1, MMP-3, and MMP-9 ELISA kits, following the manufacturer's instructions. The kits were purchased from NeoBioscience Technology Co., Ltd (Shenzhen, Guangdong, China).

*2.8.6 Determination of pro-Inflammatory cytokines*

The effects of SFP and FSFP-11 on the levels of pro-inflammatory cytokines, including IL-1β and TNF-α, were investigated by ELISA kits. The kits were purchased from NeoBioscience Technology Co. Ltd.

*2.8.7 Content of pro-collagen I α1 content in HaCaT Cells*

The effects of SFP and FSFP-11 on pro-collagen I α1 content in photodamaged HaCaT cells were investigated by ELISA kit. HaCaT cells were cultured in 6-well plates at a concentration of $6 \times 10^5$ cells per well and processed as described in Section 2.8.2. Detection was performed using a kit purchased from NeoBioscience Technology Co. Ltd.

*2.9 Quantitative reverse transcription-polymerase chain reaction (qRT–PCR) analysis*

Following the protocol in Section 2.8.1, HaCaT cells (seeded at $5\times10^5$ density) underwent PBS rinsing twice prior to harvesting, with subsequent total RNA extraction using Trizol reagent (15596026, Invitrogen, CA, USA), followed by cDNA synthesis from isolated RNA via RevertAid™ First Strand cDNA Synthesis Kit (K1622, Thermo Scientific) on a Bio-Rad T100™ Thermal Cycler for downstream qPCR analysis. Quantitative PCR amplification was performed with PowerUp™ SYBR™ Green Master Mix (Thermo Fisher Scientific, MA, USA) on a CFX Connect™ Real-Time PCR System (Model CFD3120, Bio-Rad, CA, USA), detecting transcriptional levels of: MMP-1, MMP-3, MMP-9，TNF-α, IL-1β，Pro-collagen Iα1. Using GAPDH as endogenous control (primer sequences in Table 1) The fold change in gene expression was calculated by the $2^{-\Delta\Delta CT}$ method.

**Table 1** Primer sequences of related genes

| Gene | Primer（5’-3’） | |
|---|---|---|
| *MMP-1* | Forward | CGCACAAATCCCTTCTACCC |
| | Reverse | AACAGCCCAGTACTTATTCCC |
| *MMP-3* | Forward | TTACTAGCAAGGACCTCGT |
| | Reverse | GTATCCAGCTCGTACCTCA |
| *MMP-9* | Forward | AACCAATCTCACCGACAGGCA |
| | Reverse | CAGGCCCCAGAGATTTCGACT |
| *TNF-α* | Forward | TCGAACCCCGAGTGACAAGCC |
| | Reverse | TTATCTCTCAGCTCCACGCCAT |
| *IL-1β* | Forward | AGAATGACCTGAGCACCTT |
| *Pro-collagen I α1* | Reverse | CACATAAGCCTCGTTATCCCA |
| | Forward | ATAGATGAGGCAAACATCGT |
| | Reverse | TTGTCCCAGAAACATGCCTA |

*2.10 Statistical analysis*

Triplicate experimental datasets underwent statistical processing with outcomes expressed as arithmetic mean ± SD. Data analysis was performed using one-way ANOVA with SPSS 27 software (IBM, New York, NY, USA). Statistical significance was analyzed at the level of $P < 0.05$.

## 3. Results and discussion

### *3.1 Active bacterial count and pH value*

The bacterial count and pH value of FSFPs were measured after inoculation with *Lactobacillus plantarum* at different concentrations of *Sargassum fusiforme* polysaccharides. After 1 day, the 1% concentration group reached the highest bacterial count (7.46 log CFU/mL), while the 2% and 3% groups had lower counts (7.25 and 7.01 log CFU/mL, respectively) (Fig. 1). This trend might be due to substrate inhibition at higher concentrations, which could overwhelm the bacterial enzyme system and reduce metabolic efficiency. Conversely, lower concentrations allowed more efficient utilization of polysaccharides, enhancing bacterial growth and acid production. Bacterial growth eventually slowed down in all groups, likely due to lactic acid accumulation.

The pH value showed a significant drop after 1 day of fermentation (Fig. 2). The 1% group showed the most pronounced decrease, from 6.68 to 4.42, while the control group (physiological saline) dropped from 7.15 to 3.32. The saline group's limited bacterial growth, due to the absence of a carbon source, resulted in minimal lactic acid production. However, the lack of buffering agents in saline caused a sharp pH decline even with low acid levels [36]. During post-fermentation (1-3 days), pH levels stabilized among all samples.

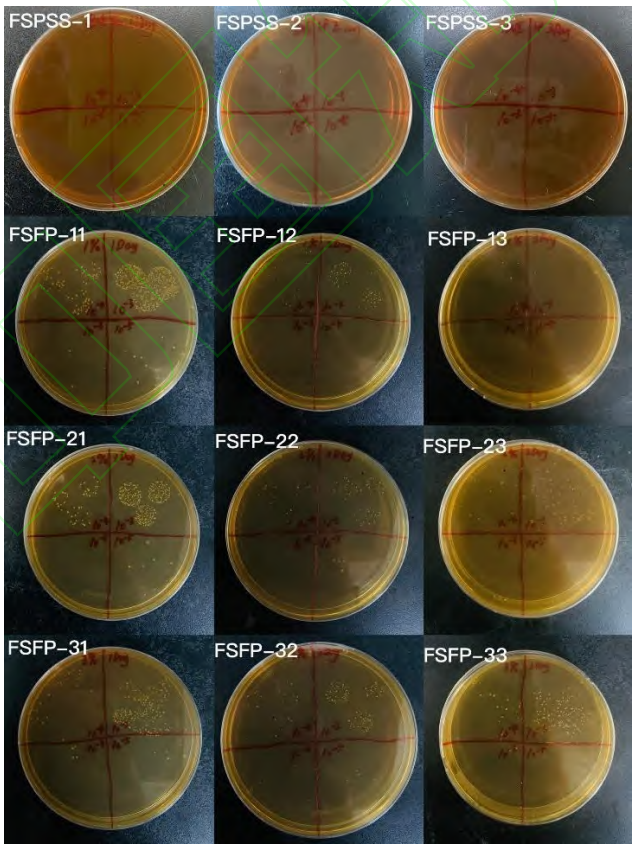


**Fig. 1.** Bacterial count (log CFU/mL) during fermentation of *Sargassum fusiforme* polysaccharides at different concentrations (1%, 2%, and 3%, respectively).

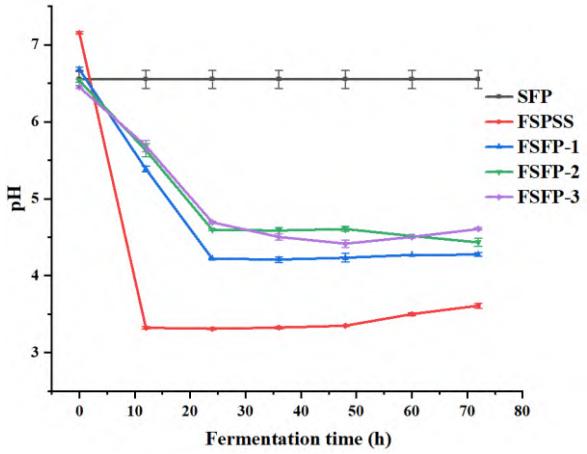


**Fig. 2.** Changes in pH values at 72 h of fermentation.

### *3.2 Chemical composition and structure*

#### *3.2.1 Chemical composition*

As shown in Table 2, SFP and FSFP contain polyphenols, proteins, reducing sugars, sulfate groups and glycuronate. Since *Sargassum fusiforme* is a brown seaweed whose chemical composition is mainly polysaccharides, the natural content of polyphenolic substances is relatively low，Li et al. isolated 42 brown algae polyphenols from Sargassum, but these polyphenols had low polymerization degrees (2-10 units) and were extracted in very small quantities, making it difficult to establish a clear relationship between them and biological activity[37]. There was a significant decrease in proteins after fermentation, except for the FSFP-31 group, while reducing sugars and sulfate groups increased to different degrees. This might be due to the fact that microorganisms might degrade proteins during the fermentation process, resulting in a decrease in protein content, whereas the fractions with higher concentrations might maintain the dynamic equilibrium of proteins [38]. Enzymes secreted by microorganisms decompose polysaccharides into monosaccharides or oligosaccharides, leading to an increase in reducing sugar content. Sulphate lyase secreted by microorganisms released sulfate groups from polysaccharides, leading to an increase in the content of free sulfate groups [39]. At the same concentration, the percentage of glycuronate in the samples increased gradually with the extension of fermentation time. Glycuronate is usually present at specific positions in polysaccharides, which is relatively stable in structure, and is not easily degraded by microorganisms. This might be because the microorganisms preferentially consumed other readily utilizable carbon sources (e.g., glucose, arabinose, etc.) during the fermentation process, whereas the glycuronate might gradually accumulate at the later stages of fermentation [40, 41].

**Table 2** Chemical compositions of SFP and FSFPs

| Sample | Total phenol（%） | Protein （%） | Reducing sugar （%） | Sulfate （%） | Glycuronate （%） |
|---|---|---|---|---|---|
| SFP | $0.88 \pm 0.01^{a}$ | $1.85 \pm 0.05^{a}$ | $3.68 \pm 0.23^{d}$ | $6.10 \pm 0.42^{d}$ | $46.61 \pm 0.98^{e}$ |
| FSFP-11 | $0.67 \pm 0.06^{c}$ | $1.63 \pm 0.03^{c}$ | $4.36 \pm 0.33^{abc}$ | $9.83 \pm 0.41^{c}$ | $48.32 \pm 0.64^{d}$ |
| FSFP-12 | $0.69 \pm 0.04^{c}$ | $1.45 \pm 0.04^{e}$ | $4.12 \pm 0.26^{bcd}$ | $9.27 \pm 0.30^{cd}$ | $51.56 \pm 0.74^{c}$ |
| FSFP-21 | $0.87 \pm 0.05^{a}$ | $1.72 \pm 0.05^{b}$ | $4.18 \pm 0.35^{bcd}$ | $10.86 \pm 0.32^{b}$ | $48.88 \pm 0.66^{d}$ |
| FSFP-22 | $0.83 \pm 0.01^{ab}$ | $1.54 \pm 0.03^{d}$ | $4.31 \pm 0.42^{ab}$ | $9.78 \pm 0.29^{c}$ | $51.21 \pm 1.03^{c}$ |
| FSFP-31 | $0.81 \pm 0.03^{b}$ | $1.80 \pm 0.03^{a}$ | $4.83 \pm 0.32^{a}$ | $12.35 \pm 0.43^{a}$ | $53.06 \pm 0.78^{b}$ |

| | | | | | |
|---|---|---|---|---|---|
| FSFP-32 | 0.84 ± 0.01$^{ab}$ | 1.63 ± 0.03$^{c}$ | 3.86 ± 0.25$^{cd}$ | 9.33 ± 0.52$^{cd}$ | 63.34 ± 0.93$^{a}$ |

Note: Different letters indicate significant difference.

### *3.2.2 Average molecular weight distribution*

The effect of fermentation on the average molecular weight of polysaccharides from *Sargassum fusiforme* is shown in Table 3 and Fig. 3. After fermentation with *Lactobacillus plantarum*, the average molecular weight of polysaccharides significantly decreased. The average molecular weight of the FSFP-12 (fermented after 2 days at 1% SFP) decreased the most by 4.03 times. It might be due to the action of polysaccharide-degrading enzymes secreted by the microorganisms during fermentation, which hydrolyze the glycosidic bonds of polysaccharides and break down large molecular polysaccharides into smaller fragments, resulting in a decrease in average molecular weight. Plant-derived lactobacilli produce organic acids during the fermentation, leading to a decrease in pH value, which would help to degrade polysaccharide.

**Table 3** The average molecular weights of SFP and FSFPs.

| Sample | Average MW (kDa) |
|---|---|
| SFP | 140.04 |
| FSFP-11 | 130.72 |
| FSFP-12 | 32.43 |
| FSFP-21 | 139.70 |
| FSFP-22 | 11.39 |
| FSFP-31 | 136.59 |
| FSFP-32 | 91.41 |

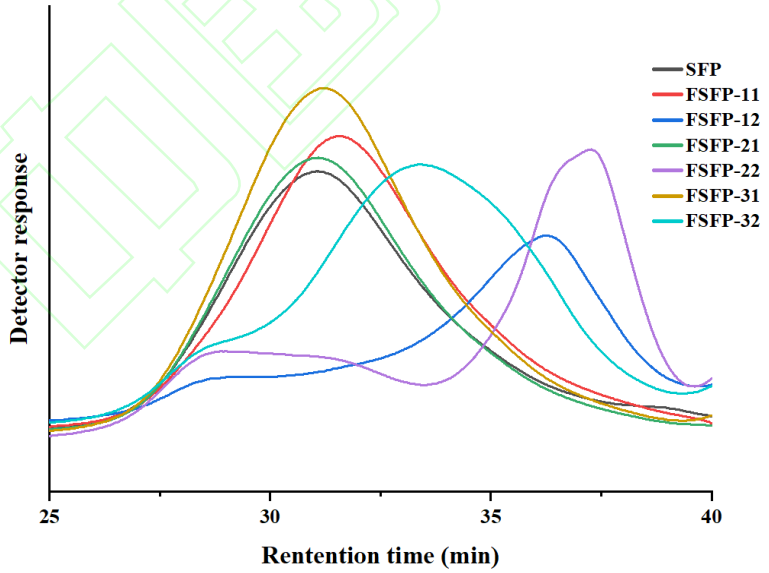


**Fig. 3.** GPC spectra of SFP and FSFPs

### *3.2.3 Monosaccharide compositions of SFP and FSFPs*

As can be seen in Fig. 4, SFP consisted of seven monosaccharides, including fucose, arabinose, galactose, glucose, xylose, galacturonic acid and glucuronic acid. Among them, glucuronic acid is the most abundant component in the monosaccharide composition. This is consistent with the results in chemical composition. The monosaccharide composition of most FSFPs remained unchanged after fermentation.

However, significant changes were observed in the molar ratios of these monosaccharides. Specifically, the molar ratio of glucuronic acid increased with prolonged fermentation time. Conversely, the molar ratios of other monosaccharides and galacturonic acid decreased. This shift likely reflects the metabolic preferences of microorganisms during fermentation. Some easily metabolized monosaccharides (e.g., glucose, arabinose) were preferentially utilized, while other less metabolizable sugars (e.g., glucuronic acid) accumulated, leading to higher molar ratios.

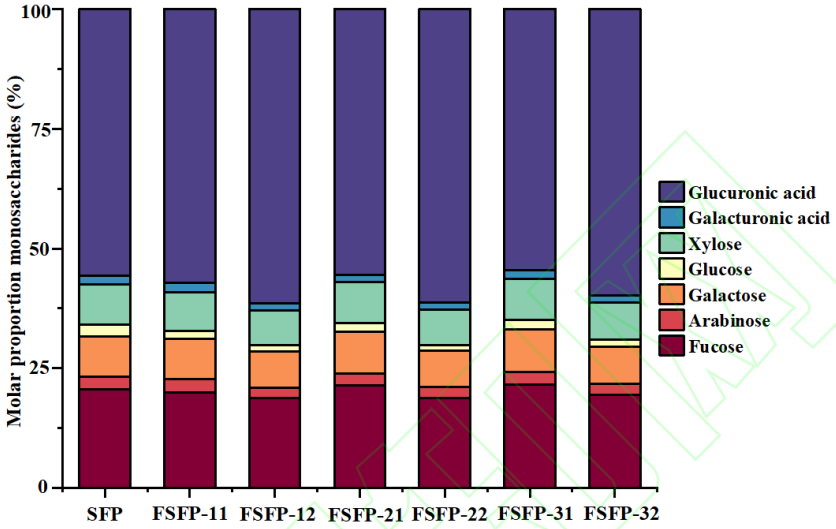


**Fig. 4.** Monosaccharide composition of SFP and FSFPs

*3.2.4 SEM analysis*

From Fig. 5, the surface morphology characteristics of SFP and FSFPs at 500 x and 2000 x can be observed. After fermentation, the surface morphology of SFP changed. The surface pores of the polysaccharide become smaller, becoming somewhat dense and smooth. The reason might be that during the fermentation, enzymes secreted by microorganisms (such as cellulase, pectinase, etc.) hydrolyzed glycosidic bonds [42], making the main chain and substituents of polysaccharides more easily to be degraded, ultimately disrupting their rough surface structure and reducing the pores on the polysaccharides surface.

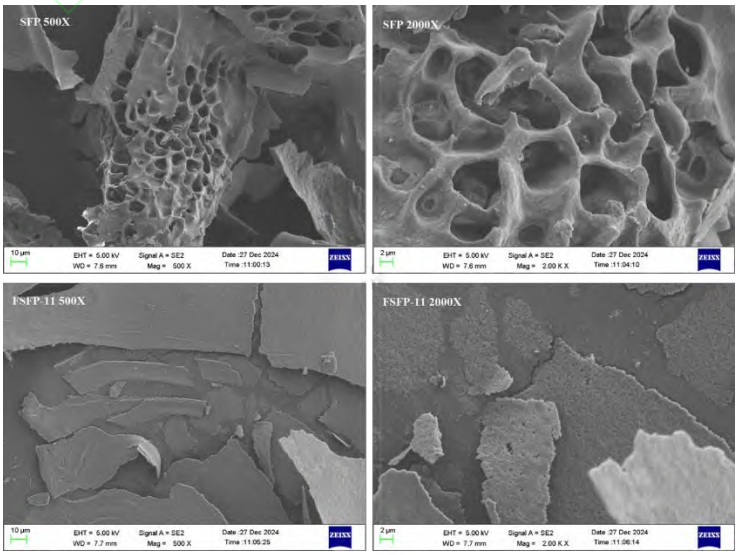

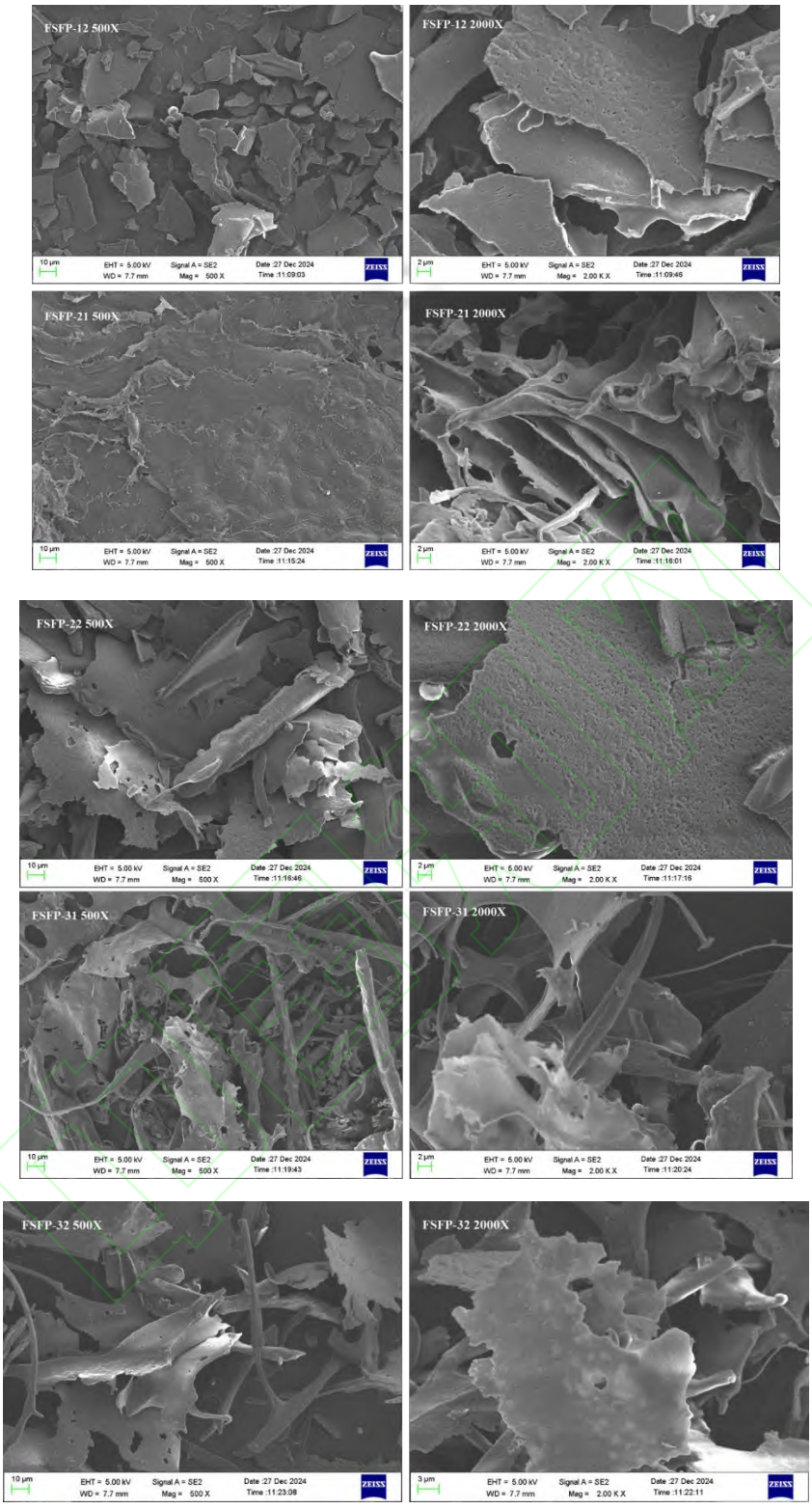


**Fig. 5.** SEM spectra of SFP and FSFPs

### *3.2.5 FTIR analysis*

As shown in Fig. 6, Fourier transform infrared spectroscopy showed that SFP and FSFPs had similar characteristic absorption peaks. This indicates that fermentation did not change the main functional groups of SFP. The broad absorption peak at 3347 $cm^{-1}$ is attributed to O-H stretching vibrations, likely originating from the hydroxyl groups of the polysaccharide. The short absorption peak of 2928 $cm^{-1}$ usually comes from the asymmetric stretching vibration of -$CH_2$-. These two characteristic functional groups are both characteristic

absorption peaks of polysaccharides. The C=O stretching vibration usually exhibits an absorption peak in the range of 1550-1650 $cm^{-1}$. So the absorption peak at 1593 $cm^{-1}$ is attributed to C=O stretching vibrations, suggesting the presence of carboxyl groups in the samples [43-45], Meanwhile, the peak at 1420 $cm^{-1}$ is associated with C-O bending vibrations, indicating the presence of uronic acid [46]. As the carboxyl group in uronic acid produces C-O-related vibrations, which are consistent with the results of monosaccharide composition and chemical composition. The characteristic absorption peaks at 1256 $cm^{-1}$ and 818 $cm^{-1}$ are generated by the stretching vibration of S-O and C-O-S bonds, respectively. The S-O bond vibration indicates the presence of sulfate groups in the sample, and the C-O-S bond stretching vibration further confirmed the connection between sulfate groups and sugar rings, indicating the presence of sulfates in the *Sargassum fusiforme* polysaccharides. The characteristic peak of β - glycosidic bond usually appears around 890-920 $cm^{-1}$, so the weak absorption peak at 900 $cm^{-1}$ is a typical characteristic peak of β - glycosidic bonds. The absorption peak near 1035 $cm^{-1}$ is related to the stretching vibration of C-O, especially the vibration of C-O-C or C-OH, which is also one of the main characteristic peaks of carbohydrates. The above results indicated that SFP and FSFPs are typical β-type polysaccharides containing uronic acid and sulfate groups. Therefore, fermentation only destroyed the glycosidic bonds of *Sargassum fusiforme* polysaccharides and did not affect the functional groups.

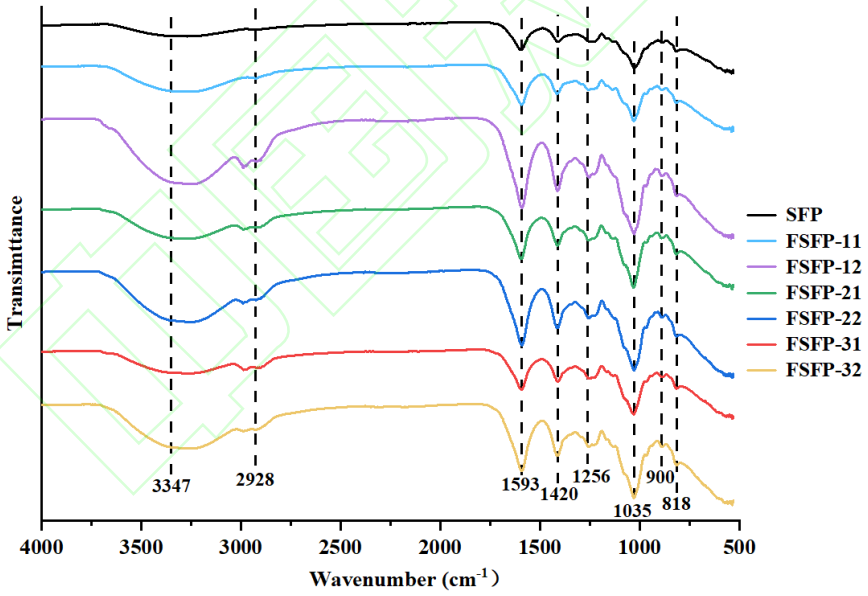


**Fig. 6.** FT-IR spectra of SFP and FSFPs

### *3.3 DPPH radical scavenging activity*

Fig. 7 demonstrates a significant enhancement in the DPPH radical scavenging activity of *Sargassum fusiforme* polysaccharides after fermentation. Notably, FSFPs group exhibited better DPPH radical scavenging activity compared with SFP. This enhancement is likely attributed to the microbial fermentation-induced cleavage of glycosidic bonds, resulting in the conversion of long-chain polysaccharides into smaller, more soluble, and biologically active low-molecular-weight fragments. These fragments exhibited increased efficiency in reacting with free radicals. However, original fermentation concentration of SFP at 2% and 3% (Fig.8b and Fig.8c) did not showed higher activities than SFP at 1%. This may be

associated with increased molecular density, stronger intermolecular interactions, and competitive inhibition among polysaccharide molecules, which collectively impair their ability to bind and scavenge DPPH radicals.

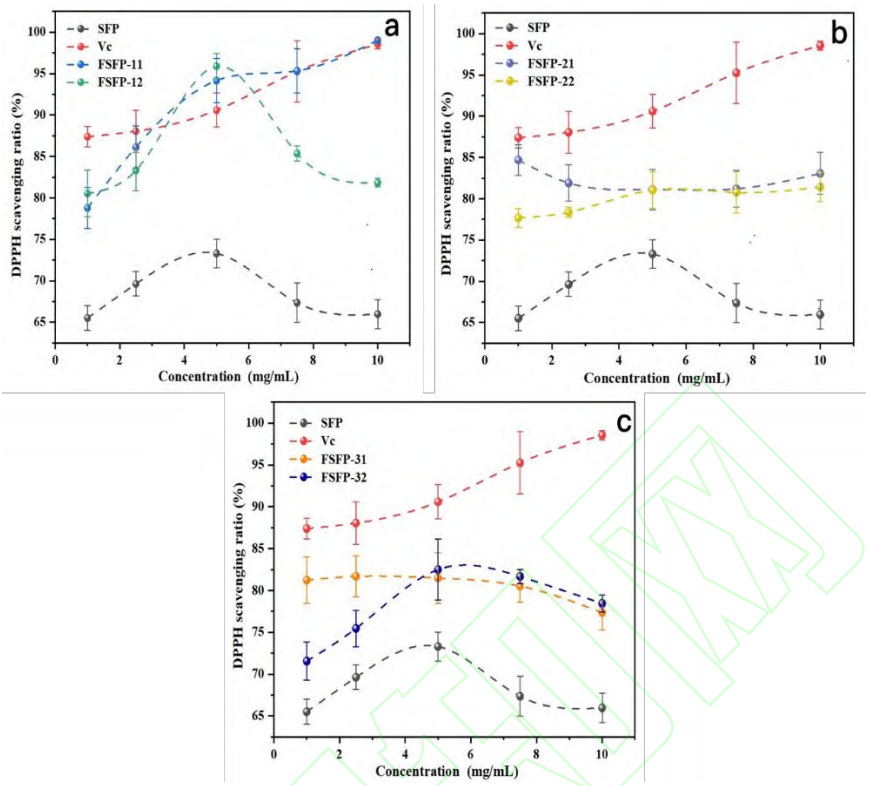


**Fig. 7.** DPPH radical scavenging abilities of SFP and FSFPs (a), FSFP-11 and FSFP-12 (b), FSFP-21 and FSFP-22 (c), FSFP-31 and FSFP-32

### *3.4 The anti-photoaging abilities of SFP and FSFPs*

#### *3.4.1 Toxicity in HaCaT cells*

A cell survival rate above 70% indicates no significant toxicity [47]. As shown in Fig. 8, all experimental groups (without UVB radiation) exhibited cell survival rates exceeding 80%, indicating that SFP and FSFPs did not have significant toxicity. Notably, FSFP-11, with the highest DPPH radical scavenging activity, significantly enhanced cell survival rates at all tested concentrations ($P < 0.001$). This effect may be attributed to its ability to scavenge free radicals and mitigate oxidative stress. These findings highlight FSFP-11's dual role in protecting cells and stimulating growth, underscoring its potential for safe and effective applications.

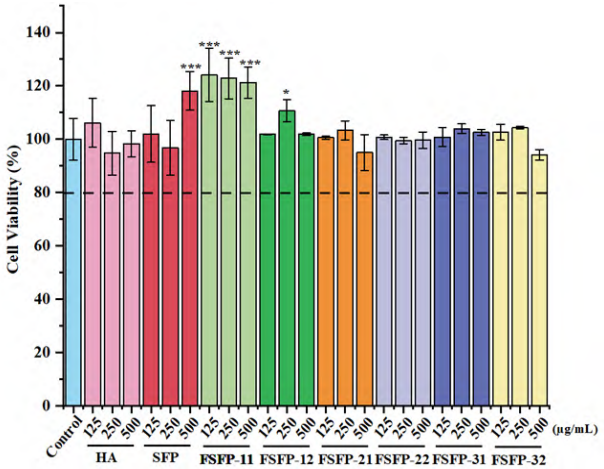


**Fig. 8.** Toxicity of SFP and FSFPs on HaCaT cells. ***$P < 0.001$.

### 3.4.2 Survival rate of HaCaT cells

Photoaging, characterized by structural and functional damage to skin tissues, results from prolonged UV radiation exposure. This study evaluated the anti-photoaging potential of SFP and FSFPs by using UVB-irradiated HaCaT cells. Fig. 9 demonstrated that UVB exposure significantly reduced cell viability in the model group compared to the control group ($P < 0.001$), confirming successful establishment of the photoaging model. Treated with HA, FSFP-11, FSFP-21, FSFP-31, and FSFP-32 significantly enhanced cell survival ($P < 0.001$), while SFP showed no notable effect, indicating that fermentation markedly improved the anti-photoaging activity of *Sargassum fusiforme* polysaccharides.

At 250 μg/mL, FSFP-11 exhibited the strongest anti-photoaging activity ($P < 0.001$). However, at 500 μg/mL, cell viability declined in all groups except SFP, FSFP-22, and FSFP-31. This reduction likely stems from the samples exceeding cellular tolerance limits, increasing oxidative stress and inflammatory responses, thereby diminishing their protective effects against photoaging [48, 49].

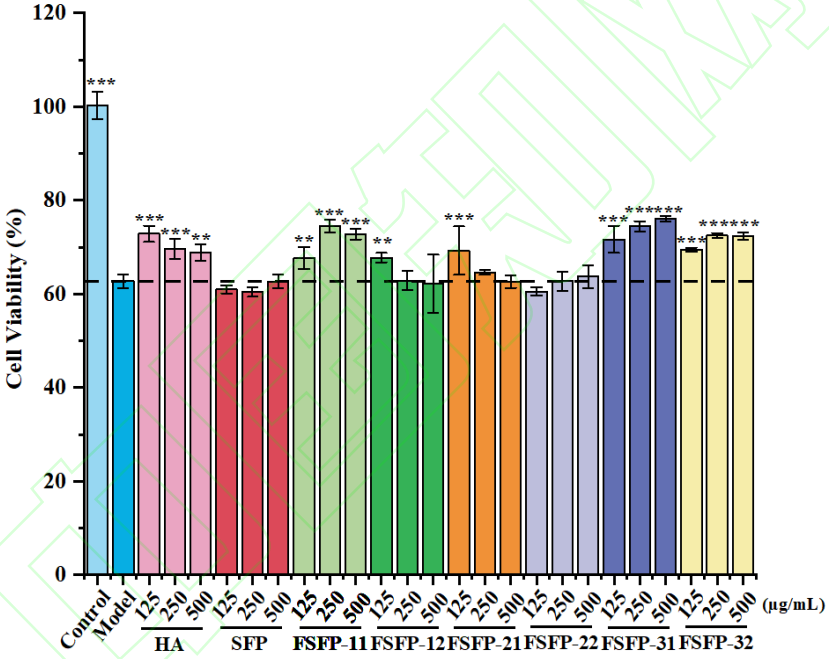


**Fig. 9.** Effects of SFP and FSFPs on cell viability of photoaged HaCaT cells. $^{**}P < 0.01$, $^{***}P < 0.001$

### 3.4.3 Hydroxyproline (HYP) levels in HaCaT cells

Hydroxyproline (HYP), located between collagen and elastin, stabilizes collagen's triple helix, enhancing skin elasticity and moisture [50]. Post-irradiation, the model group exhibited a significant HYP secretion drop ($P < 0.001$) compared to the control group, confirming successful photodamage modeling and inhibited collagen synthesis. FSFP-11, and FSFP-32 groups showed higher HYP levels ($P < 0.001$), compared with the SFP group. This indicates that fermented polysaccharides could effectively enhance collagen synthesis and resist photoaging than non-fermented polysaccharides. FSFP-11, in particular, outperformed both the control and positive groups, showing a 46.2% HYP increase over the model group, highlighting its superior anti-photoaging activity. Therefore, FSFP-11 was selected for further study.

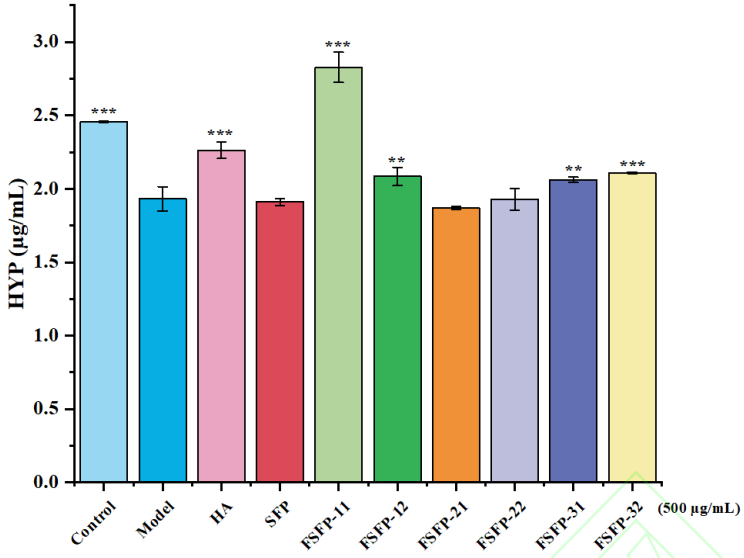


**Fig. 10.** Effects of SFP and FSFPs on HYP levels in HaCaT cells. $^{**}P < 0.01$, $^{***}P < 0.001$

*3.4.4 MMP-1, MMP-3 and MMP-9 levels*

The MMP (matrix metalloproteinase) family comprises zinc- and calcium-dependent proteases that degrade extracellular matrix (ECM) components, playing critical roles in tissue remodeling [51], wound healing, and angiogenesis [52]. Specifically, MMP-1 overexpression degrades collagen, leading to wrinkle formation [53], while MMP-3 targets proteoglycans, fibronectin, laminin, and type IV collagen, and activates other MMPs like MMP-1 and MMP-9 [54]. MMP-9 primarily degrades type IV collagen and gelatin [55]. These enzymes are pivotal in skin disease progression and are potential therapeutic targets.

In our study, UVB irradiation significantly increased the levels of MMP-1, MMP-3 and MMP-9 ($P < 0.001$) in the model group, successfully establishing a photoaging model. FSFP-11, SFP and HA all significantly inhibited MMP-1 ($P < 0.001$). Notably, FSFP-11 exhibited a stronger inhibitory effect on MMP-1 than the positive control, indicating its potential for anti-photoaging activity. Furthermore, FSFP-11 exhibited the strongest inhibitory effects on MMP-3 and MMP-9. At a concentration of 250 μg/mL, inhibition rates of 38.8% and 48.1% were observed for MMP-3 and MMP-9, respectively. The overall inhibitory effect on all three MMPs was optimal at this concentration. This may be because FSFP-11 interacts more effectively with cell surface receptors or signaling molecules, thereby significantly inhibiting MMP expression.

*3.4.5 IL-1β and TNF-α levels*

Skin diseases are closely linked to pro-inflammatory factors, which play a pivotal role in the pathogenesis of inflammatory skin conditions by mediating inflammatory responses, immune modulation, and tissue damage. IL-1β is a central regulator of inflammatory responses, particularly in autoinflammatory diseases [56]. It is synthesized as an inactive precursor (pro-IL-1β) and requires cleavage by inflammasomes and caspase-1 to become active [57]. IL-1β not only induces the expression of other pro-inflammatory factors like TNF-α [58] but also promotes tissue destruction by upregulating matrix metalloproteinases (MMPs) during

chronic or excessive inflammation [59]. TNF-α, a 157-amino acid protein that functions as a homotrimer, exists initially as a transmembrane precursor (tmTNF) [60] UV radiation activates the NF-κB and AP-1 signaling pathways, leading to TNF-α expression and release [61].

In our study, UV irradiation significantly upregulated IL-1β levels in the model group compared to the control group, indicating irradiation-induced damage to HaCaT cells. Both FSFP-11 and SFP significantly reduced the IL-1β levels at 125 μg/mL and 500 μg/mL, respectively. Notably, FSFP-11 exhibited the strongest anti-inflammatory activity, reducing IL-1β levels by 70.8% at 500 μg/mL compared to the model group. This suggests that fermented *Sargassum fusiforme* polysaccharide (FSFP-11) is more effective in inhibiting IL-1β secretion and mitigating inflammatory damage in HaCaT cells indicating its potent anti-photoaging activity.

As shown in Fig. 11d, UVB irradiation significantly increased TNF-α levels in the model group compared to the control group ($P < 0.001$). Pretreatment with SFP, FSFP-11, and HA significantly reduced TNF-α levels ($P < 0.001$). Notably, FSFP-11 at 125 μg/mL decreased TNF-α levels by 46.0%. These results demonstrate that FSFP-11 effectively mitigated photoaging by suppressing pro-inflammatory cytokine secretion. Moreover, FSFP-11 showed better inhibition effects on TNF-α level, compared with SFP, suggesting that fermentation could enhance the anti-inflammatory properties of *Sargassum fusiforme* polysaccharides.

*3.4.6 Pro-collagen I α1 levels*

Pro-collagen I α1 is essential for maintaining the skin's structural integrity, elasticity, and mechanical strength. UV irradiation activates matrix metalloproteinases (MMPs), which degrade collagen and elastin fibers and reduce Pro-collagen I α1 synthesis by regulating the TGF-β/Smad signaling pathway [62]. Thus, Pro-collagen I α1 level could reflect the photoaging resistance.

Fig. 11f shows that the model group secreted significantly less pro-collagen Iα1 than the Control group ($P < 0.001$), indicating that UV radiation severely impairs HaCaT cells' ability to synthesize and secrete pro-collagen I α1, further confirming its detrimental effect on skin collagen metabolism. In contrast, the sample groups treated with SFP, FSFP-11, and HA exhibited significantly higher Pro-collagen I α1 secretion than the model group, demonstrating their ability to counteract UV-induced collagen synthesis inhibition. Notably, the pro-collagen I α1 levels in the Sample group were 2.3 to 3 times higher than those in the control group, suggesting these treatments not only repaired UV-induced damage but also enhanced collagen synthesis. Importantly, FSFP-11 showed a stronger pro-collagen I α1 synthesis capacity than SFP, indicating that fermentation could enhance the anti-photoaging activity of *Sargassum fusiforme* polysaccharides.

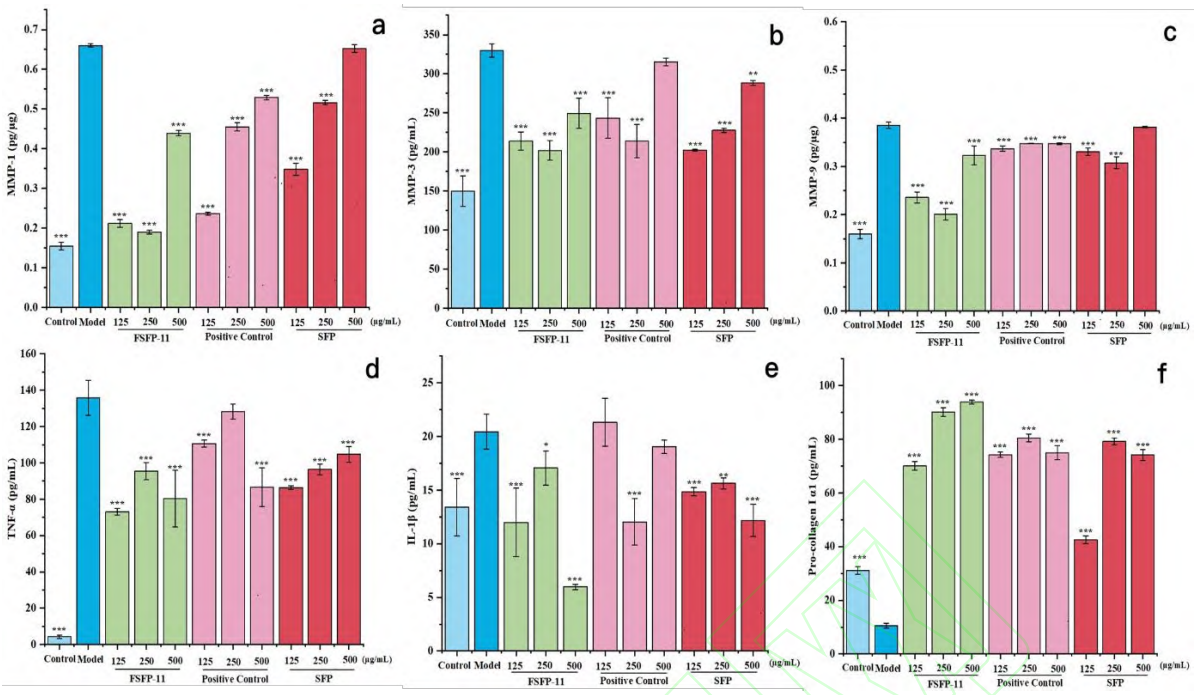


**Fig. 11.** The levels of anti-photoaging and anti-inflammatory indexes in cells

(a) MMP-1 level, (b) MMP-3 level, (c) MMP-9 level, (d) TNF-α level, (e) IL-1β level, (f) Pro-collagen I α1 level. *$P < 0.05$, **$P < 0.01$, ***$P < 0.001$

### *3.5 Effect of SFP and FSFPs on the gene expression of MMP-1, MMP-3, MMP-9, TNF-α, IL-1β and Pro-collagen I α1*

As shown in Fig.12a-c, photodamage assessment revealed marked upregulation of MMP-1, MMP-3, and MMP-9 in UVB-exposed models ($P < 0.001$), implicating enhanced matrix metalloproteinase activity in photoaging-associated extracellular matrix degradation. Compared with the model group, FSFP-11 significantly downregulated the gene expression levels of MMP-1, MMP-3, and MMP-9 in HaCaT cells ($P < 0.001$). Under the intervention of FSFP-11 at a dose of 250 μg/mL, the relative gene expression levels of MMP-1, MMP-3, and MMP-9 in HaCaT cells were reduced by 47.1%、58.8% and 67.2%, respectively, compared to the model group.

As shown in Fig.12e, the gene expression level of IL-1β in the model group was significantly higher than that in the control group, indicating that UVB irradiation triggered cellular inflammatory responses. Compared with the model group, both FSFP-11 and SFP down-regulated the gene expression level of IL-1β in HaCaT cells. Under the intervention of 250 and 500 μg/mL doses, FSFP-11 decreased IL-1β by 41.2% and 51.3%, respectively, compared with the model group. SFP decreased by 30.4% and 34.3%, respectively, compared with the model group. The relative gene expression level of IL-1β in HaCaT cells by FSFP-11 was better than that of SFP. This indicated that fermentation-treated polysaccharides could enhance anti-inflammatory activity. Based on the above results, the anti-photoaging activity of FSFP-11 was further verified by results in the expression of photoaging-related genes.

As shown in Fig.12, in HaCaT cells, UV irradiation treatment significantly down-regulated the gene expression of Pro-collagen I α1, whereas FSFP-11 and SFP could promote their expression levels. Moreover,

FSFP-11 could better up-regulate the gene expression compared with an equal dose of SFP. Thus, these results further suggested that FSFP-11 had better anti-photoaging activity.

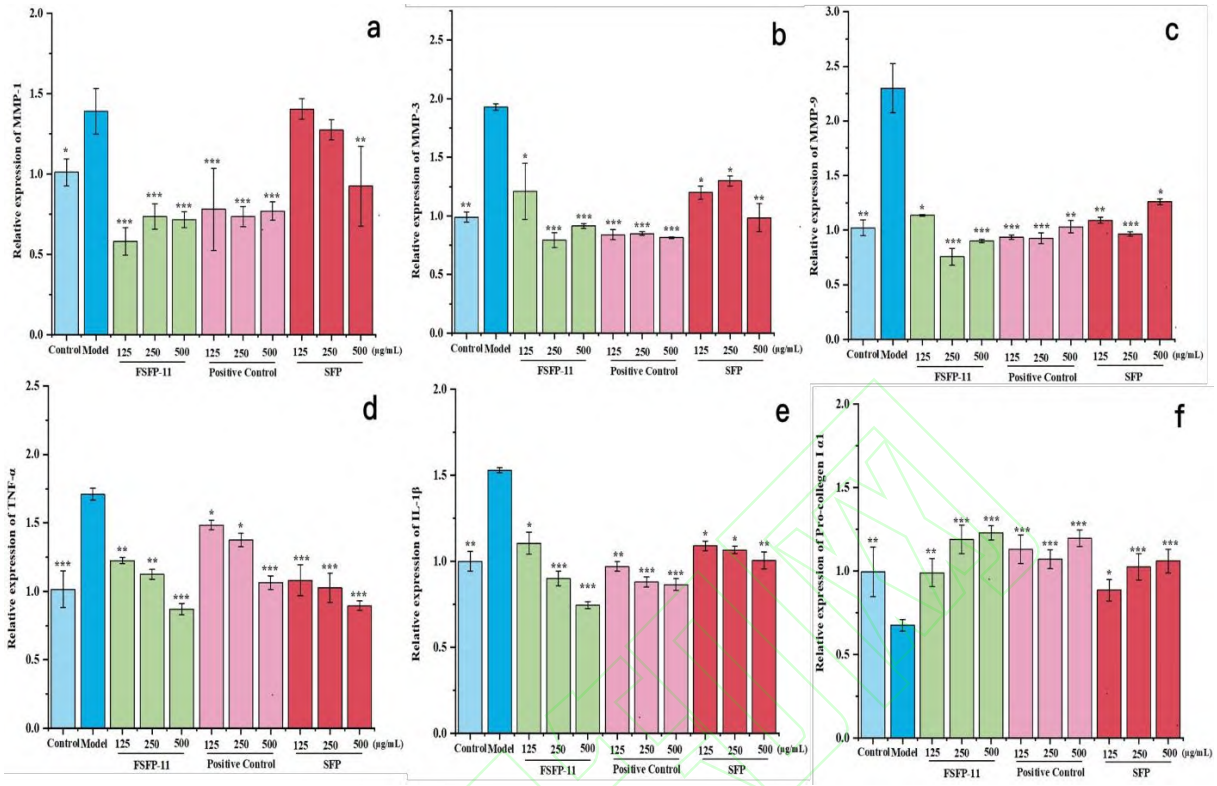


**Fig. 12.** Effects of SFP and FSFPs on the gene expressions in photoaged HaCaT cells

(a) MMP-1 level, (b) MMP-3 level, (c) MMP-9 level, (d) TNF-α level, (e) IL-1β level, (f) Pro-collagen I α1 level. $*P < 0.05$, $**P < 0.01$, $***P < 0.001$

## 4. Conclusions

This study compared the structural characteristic and anti-photoaging activities of *Sargassum fusiforme* polysaccharides before and after fermented with *Lactobacillus plantarum*. During fermentation, some of the glycosidic bonds in SFP broke down, resulting in a significant reduction in molecular weight (75.2%) and an altered ratio of monosaccharide compositions (an increase in glucuronic acid and a decrease in fucose). However, the polysaccharide's main functional group structural characteristics remained unchanged. Therefore, SFP and FSFPs have a similar primary structure; both are β-type sulfated polysaccharides containing sulfate groups and glucuronic acid. This structural feature gives both materials high anion density due to the synergistic action of the carboxylate and sulfate groups. Additionally, the surface morphology of the FSFPs changed after fermentation. The pores on the polysaccharide surface became smaller and more densely packed, resulting in a smoother surface. *In vitro* experiments using UVB-irradiated HaCaT cells showed that fermented polysaccharides showed better anti-photoaging activities, compared with non-fermented polysaccharide. Fermented polysaccharides significantly increased cell viability and collagen synthesis (the levels of HYP and pro-collagen I α1), and reduced collagen degradation by decreasing the levels and gene expressions of MMP-1, MMP-3, and MMP-9. Additionally, fermented polysaccharide FSFP-11 effectively inhibited the production and gene expressions of IL-1β and TNF-α. These findings suggest that fermentation

could enhance the anti-photoaging activity of seaweed polysaccharides, and could be a developed as a prospect way to degrade polysaccharide. Future studies could use a combined analysis strategy that integrates metabolomics and transcriptomics with an in-depth analysis of polysaccharide structure to systematically elucidate the molecular mechanism by which fermentation enhances the anti-photoaging activity of Sargassum polysaccharides.

## Disclosure statement

The authors declare no conflict of interest.

## Acknowledgments

This work was supported by the National Key Research and Development Program of China (2024YFF1106000, 2024YFE0109500), the Guangdong Basic and Applied Basic Research Foundation (2023B1515040014), Guangdong Science and Technology Plan Projects (2023A0505050117), the National Natural Science Foundation of China (22278153), and 111 Project (B17018).

## References

[1] S.W. Kang, G.J. Fisher, J.J. Voorhees, Photoaging - Pathogenesis, prevention, and treatment, Clinics in Geriatric Medicine. 17 (2001) 643-+. https://doi.org/10.1016/s0749-0690(05)70091-4.

[2] A. Leandro, L. Pereira, A.M.M. Gonçalves, Diverse Applications of Marine Macroalgae, Marine Drugs. 18 (2020) 17. https://doi.org/10.3390/md18010017.

[3] N. Flórez-Fernández, A. Rodríguez-Coello, T. Latire, et al., Anti-inflammatory potential of ulvan, International Journal of Biological Macromolecules. 253 (2023) 126936. https://doi.org/10.1016/j.ijbiomac.2023.126936.

[4] Saraswati, P.E. Giriwono, D. Iskandriati, et al., *Sargassum* Seaweed as a Source of Anti-Inflammatory Substances and the Potential Insight of the Tropical Species: A Review, Marine Drugs. 17 (2019) 590. https://doi.org/10.3390/md17100590.

[5] L. Song, Y.Z. Niu, R. Chen, et al., A Comparative Analysis of the Anti-Tumor Activity of Sixteen Polysaccharide Fractions from Three Large Brown Seaweed, *Sargassum horneri*, *Scytosiphon lomentaria*, and *Undaria pinnatifida*, Marine Drugs. 22 (2024) 316. https://doi.org/10.3390/md22070316.

[6] J.X. Xu, W. Liao, S.X. Yang, et al., *Ulva lactuca* polysaccharide inhibits hepatocellular carcinoma growth by induces the expression of CD5L and activates complement cascade, Journal of Functional Foods. 112 (2024) 105994. https://doi.org/10.1016/j.jff.2023.105994.

[7] K. Takeda, K. Tomimori, R. Kimura, et al., Anti-tumor activity of fucoidan is mediated by nitric oxide released from macrophages, International Journal of Oncology. 40 (2012) 251-260. https://doi.org/10.3892/ijo.2011.1168.

[8] M. Schepers, N. Martens, A. Tiane, et al., Edible seaweed-derived constituents: an undisclosed source of neuroprotective compounds, Neural Regeneration Research. 15 (2020) 790-795. https://doi.org/10.4103/1673-5374.268894.

[9] C.S. Shi, Y.X. Sang, G.Q. Sun, et al., Characterization and bioactivities of a novel polysaccharide obtained from *Gracilariopsis lemaneiformis*, Anais Da Academia Brasileira De Ciencias. 89 (2017) 175-189. https://doi.org/10.1590/0001-3765201720160488.

[10] Y.N. Li, E. McGowan, S.Z. Chen, et al., Immunopotentiating Activity of Fucoidans and Relevance to Cancer Immunotherapy, Marine Drugs. 21 (2023) 128. https://doi.org/10.3390/md21020128.

[11] M. Pérez-Recalde, M.C. Matulewicz, C.A. Pujol, et al., *In vitro* and *in vivo* immunomodulatory activity of sulfated polysaccharides from red seaweed *Nemalion helminthoides*, International Journal of Biological Macromolecules. 63 (2014) 38-42. https://doi.org/10.1016/j.ijbiomac.2013.10.024.

[12] J.D. Barbosa, D.A. Sabry, C.H.F. Silva, et al., Immunostimulatory Effect of Sulfated Galactans from the Green Seaweed *Caulerpa cupressoides* var. *flabellata*, Marine Drugs. 18 (2020) 234. https://doi.org/10.3390/md18050234.

[13] M.A.P. Panjaitan, R.D. Kasitowati, N. Putri, et al., Polysaccharide isolation of Brown seaweed: Sargassum sp and its photoprotection activity, IOP Conf. Ser., Earth Environ. Sci. (UK). 1036 (2022) 012039 (012036 pp.)-012039 (012036 pp.). https://doi.org/10.1088/1755-1315/1036/1/012039.

[14] V. Jesumani, H. Du, P.B. Pei, et al., Comparative study on skin protection activity of polyphenol-rich extract and polysaccharide-rich extract from *Sargassum vachellianum*, Plos One. 15 (2020) e0227308. https://doi.org/10.1371/journal.pone.0227308.

[15] R. Zhang, X.X. Zhang, Y.X. Tang, et al., Composition, isolation, purification and biological activities of *Sargassum fusiforme* polysaccharides: A review, Carbohydrate Polymers. 228 (2020) 115381. https://doi.org/10.1016/j.carbpol.2019.115381.

[16] S. Zhang, L. Chen, N. Shang, et al., Recent Advances in the Structure, Extraction, and Biological Activity of *Sargassum fusiforme* Polysaccharides, Marine Drugs. 23 (2025) 98. https://doi.org/10.3390/md23030098.

[17] A.K. Patel, A.P. Vadrale, R.R. Singhania, et al., Algal polysaccharides: current status and future prospects, Phytochemistry Reviews. 22 (2023) 1167-1196. https://doi.org/10.1007/s11101-021-09799-5.

[18] A. Karlsson, S.K. Singh, Acid hydrolysis of sulphated polysaccharides. Desulphation and the effect on molecular mass, Carbohydrate Polymers. 38 (1999) 7-15. https://doi.org/10.1016/s0144-8617(98)00085-x.

[19] S.T. Merino, J. Cherry. Progress and challenges in enzyme development for Biomass utilization. In: Olsson L., editor Biofuels. 2007, p. 95-120. https://doi.org/10.1007/10_2007_066.

[20] F. Chemat, N. Rombaut, A.G. Sicaire, et al., Ultrasound assisted extraction of food and natural products. Mechanisms, techniques, combinations, protocols and applications. A review, Ultrasonics Sonochemistry. 34 (2017) 540-560. https://doi.org/10.1016/j.ultsonch.2016.06.035.

[21] J.L. Nie, X.T. Fu, L. Wang, et al., A systematic review of fermented *Saccharina japonica*: Fermentation conditions, metabolites, potential health benefits and mechanisms, Trends in Food Science & Technology. 123 (2022) 15-27. https://doi.org/10.1016/j.tifs.2022.03.001.

[22] Z. Wang, Y. Zheng, Z. Lai, et al., Effect of Saccharomyces cerevisiae CICC 32883 Fermentation on the Structural Features and Antioxidant Protection Effect of Chinese Yam Polysaccharide, Foods. (2025), https://doi.org/10.3390/foods14040564

[23] Z. Qu, H. Liu, J. Yang, et al., Selective utilization of medicinal polysaccharides by human gut Bacteroides and Parabacteroides species, Nat Commun. 16 (2025) 638. https://doi.org/10.1038/s41467-025-55845-7.

[24] J. Yu, Z. Hu, E. Yan, et al., Structure modification and bioactivity improvement of crude polysaccharides extracted from white hyacinth beans after fermentation by different bacteria, Biomass Conversion and Biorefinery. (2025) https://doi.org/10.1007/s13399-025-06636-z.

[25] W.Z. Yao, M.Y. Liu, X.Y. Chen, et al., Effects of UV/$H_2O_2$ degradation and step gradient ethanol precipitation on *Sargassum fusiforme* polysaccharides: Physicochemical characterization and protective effects against intestinal epithelial injury, Food Research International. 155 (2022) 111093. https://doi.org/10.1016/j.foodres.2022.111093.

[26] C. Wang, X.D. Gao, R.K. Santhanam, et al., Effects of polysaccharides from *Inonotus obliquus* and its chromium (III) complex on advanced glycation end-products formation, α-amylase, α-glucosidase activity and $H_2O_2$-induced oxidative damage in hepatic L02 cells, Food and Chemical Toxicology. 116 (2018) 335-345. https://doi.org/10.1016/j.fct.2018.04.047.

[27] T. Bitter, H.M. Muir, A modified uronic acid carbazole reaction, Analytical biochemistry. 4 (1962) 330-334. https://doi.org/10.1016/0003-2697(62)90095-7.

[28] X.Y. Chen, L.J. You, Y.X. Ma, et al., Influence of UV/H2O2 treatment on polysaccharides from *Sargassum fusiforme*: Physicochemical properties and RAW 264.7 cells responses, Food and Chemical Toxicology. 153 (2021) 112246. https://doi.org/10.1016/j.fct.2021.112246.

[29] K.S. Dodgson, R.G. Price, A note on the determination of the ester sulphate content of sulphated polysaccharides, The Biochemical journal. 84 (1962) 106-110. https://doi.org/10.1042/bj0840106.

[30] T. Gagic, Z. Knez, M. Skerget, Subcritical Water Extraction of Chestnut Bark and Optimization of Process Parameters, Molecules. 25 (2020) 2774. https://doi.org/10.3390/molecules25122774.

[31] H. Lindsay, A colorimetric estimation of reducing sugars in potatoes with 3,5-dinitrosalicylic acid, Potato Research. 16 (1973) 176-179. https://doi.org/10.1007/BF02356048.

[32] S.Y. Chang, X.Y. Chen, Y.F. Chen, et al., UV/$H_2O_2$-Degraded Polysaccharides from *Sargassum fusiforme*: Purification, Structural Properties, and Anti-Inflammatory Activity, Marine Drugs. 21 (2023) 561. https://doi.org/10.3390/md21110561.

[33] X. Li, S.M. Huang, X. Chen, et al., Structural characteristic of a sulfated polysaccharide from *Gracilaria Lemaneiformis* and its lipid metabolism regulation effect, Food & Function. 11 (2020) 10876-10885. https://doi.org/10.1039/d0fo02575e.

[34] T. Yamaguchi, H. Takamura, T. Matoba, et al., HPLC method for evaluation of the free radical-scavenging activity of foods by using 1,1-diphenyl-2-picrylhydrazyl, Bioscience Biotechnology and Biochemistry. 62 (1998) 1201-1204. https://doi.org/10.1271/bbb.62.1201.

[35] D.S. Ji, L.J. You, Y.L. Ren, et al., Protective effect of polysaccharides from *Sargassum fusiforme* against UVB-induced oxidative stress in HaCaT human keratinocytes, Journal of Functional Foods. 36 (2017) 332-340. https://doi.org/10.1016/j.jff.2017.06.051.

[36] A. Hlas, V. Ganesh, J. Marks, et al., Buffering Mitigates Chondrocyte Oxidative Stress, Metabolic Dysfunction, and Death Induced by Normal Saline: Formulation of a Novel Arthroscopic Irrigant, International Journal of Molecular Sciences. 25 (2024) 1286. https://doi.org/10.3390/ijms25021286.

[37] Y.X. Li, I. Wijesekara, Y. Li, et al., Phlorotannins as bioactive agents from brown algae, Process Biochemistry. 46 (2011) 2219-2224. https://doi.org/10.1016/j.procbio.2011.09.015.

[38] C. Woern, L. Grossmann, Microbial gas fermentation technology for sustainable food protein production, Biotechnology Advances. 69 (2023) 108240. https://doi.org/10.1016/j.biotechadv.2023.108240.

[39] D.M. van Vliet, S. Palakawong Na Ayudthaya, S. Diop, et al., Anaerobic Degradation of Sulfated Polysaccharides by Two Novel Kiritimatiellales Strains Isolated From Black Sea Sediment, Front Microbiol. 10 (2019) 253. https://doi.org/10.3389/fmicb.2019.00253.

[40] Q. Li, L. Liu, J.H. Zhang, et al., Effects of pile fermentation on the physicochemical, functional, and biological properties of tea polysaccharides, Food Chemistry. 410 (2023) 135353. https://doi.org/10.1016/j.foodchem.2022.135353.

[41] X. Wang, K. Xia, X. Yang, et al., Growth strategy of microbes on mixed carbon sources, Nat Commun. 10 (2019) 1279. https://doi.org/10.1038/s41467-019-09261-3.

[42] N. Karaki, A. Aljawish, C. Humeau, et al., Enzymatic modification of polysaccharides: Mechanisins, properties, and potential applications: A review, Enzyme and Microbial Technology. 90 (2016) 1-18. https://doi.org/10.1016/j.enzmictec.2016.04.004.

[43] G.D. Manrique, F.M. Lajolo, FT-IR spectroscopy as a tool for measuring degree of methyl esterification in pectins isolated from ripening papaya fruit, Postharvest Biology and Technology. 25 (2002) 99-107. Pii s0925-5214(01)00160-0. https://doi.org/10.1016/s0925-5214(01)00160-0.

[44] J.H. Hu, W.Z. Yao, S.Y. Chang, et al., Structural characterization and anti-photoaging activity of a polysaccharide from *Sargassum fusiforme*, Food Research International. 157 (2022) 111267. https://doi.org/10.1016/j.foodres.2022.111267.

[45] T. Hong, J.Y. Yin, S.P. Nie, et al., Applications of infrared spectroscopy in polysaccharide structural analysis: Progress, challenge and perspective, Food Chem X. 12 (2021) 100168. https://doi.org/10.1016/j.fochx.2021.100168.

[46] C. Cui, J.H. Lu, D. Sun-Waterhouse, et al., Polysaccharides from *Laminaria japonica*: Structural characteristics and antioxidant activity, Lwt-Food Science and Technology. 73 (2016) 602-608. https://doi.org/10.1016/j.lwt.2016.07.005.

[47] X.M. Liu, D.P. Rodeheaver, J.C. White, et al., A comparison of in vitro cytotoxicity assays in medical device regulatory studies, Regulatory Toxicology and Pharmacology. 97 (2018) 24-32. https://doi.org/10.1016/j.yrtph.2018.06.003.

[48] C. Shen, Z. Luo, S. Ma, et al., Microbe-Derived Antioxidants Protect IPEC-1 Cells from $H_2O_2$-Induced Oxidative Stress, Inflammation and Tight Junction Protein Disruption via Activating the Nrf2 Pathway to Inhibit the ROS/NLRP3/IL-1β Signaling Pathway, Antioxidants. 13 (2024) 533. https://doi.org/10.3390/antiox13050533.

[49] M. Požgajová, A. Navrátilová, M. Kovár, et al. Cell Protection by Oxidative Stress Mitigation Using Substances with Bioactive Properties. In: Novo Barros A., A.C. Santos Abra ão, editors. The Power of Antioxidants - Unleashing Nature's Defense Against Oxidative Stress. Rijeka: IntechOpen; 2024. https://doi.org/10.5772/intechopen.1004522.

[50] K. Mizuno, T. Hayashi, D.H. Peyton, et al., Hydroxylation-induced stabilization of the collagen triple helix -: Acetyl-(glycyl-4(*R*)-hydroxyprolyl-4(*R*)-hydroxyprolyl) $_{10}$-$NH_2$ forms a highly stable triple helix, Journal of Biological Chemistry. 279 (2004) 38072-38078. https://doi.org/10.1074/jbc.M402953200.

[51] C. Milaras, P. Lepetsos, D. Dafou, et al., Association of Matrix Metalloproteinase (MMP) Gene Polymorphisms With Knee Osteoarthritis: A Review of the Literature, Cureus. 13 (2021) e18607. https://doi.org/10.7759/cureus.18607.

[52] P. Pittayapruek, J. Meephansan, O. Prapapan, et al., Role of Matrix Metalloproteinases in Photoaging and Photocarcinogenesis, International Journal of Molecular Sciences. 17 (2016) 868. https://doi.org/10.3390/ijms17060868.

[53] S.M. Eck, J.S. Blackburn, A.C. Schmucker, et al., Matrix metalloproteinase and G protein coupled receptors: Co-conspirators in the pathogenesis of autoimmune disease and cancer, Journal of Autoimmunity. 33 (2009) 214-221. https://doi.org/10.1016/j.jaut.2009.09.011.

[54] C. Zhang, L. Chen, Y. Gu, Polymorphisms of *MMP-1* and *MMP-3* and susceptibility to rheumatoid arthritis A meta-analysis, Zeitschrift Fur Rheumatologie. 74 (2015) 258-262. https://doi.org/10.1007/s00393-014-1537-2.

[55] M. Borg, S. Brincat, G. Camilleri, et al., The role of cytokines in skin aging, Climacteric. 16 (2013) 514-521. https://doi.org/10.3109/13697137.2013.802303.

[56] C.A. Dinarello, The IL-1 family of cytokines and receptors in rheumatic diseases, Nature Reviews Rheumatology. 15 (2019) 612-632. https://doi.org/10.1038/s41584-019-0277-8.

[57] H. Zhang, Anti-IL-1beta therapies, Recent patents on DNA & gene sequences. 5 (2011) 126-135. https://doi.org/10.2174/187221511796392024.

[58] K. Pocino, V. Carnazzo, A. Stefanile, et al., Tumor Necrosis Factor-Alpha: Ally and Enemy in Protean Cutaneous Sceneries, International Journal of Molecular Sciences. 25 (2024) 7762. https://doi.org/10.3390/ijms25147762.

[59] A. Honda, R. Abe, T. Makino, et al., Interleukin-1β and macrophage migration inhibitory factor (MIF) in dermal fibroblasts mediate UVA-induced matrix metalloproteinase-1 expression, Journal of Dermatological Science. 49 (2008) 63-72. https://doi.org/10.1016/j.jdermsci.2007.09.007.

[60] A. Makos, J.H. Kuiper, O. Kehoe, et al., Psoriatic arthritis: review of potential biomarkers predicting response to TNF inhibitors, Inflammopharmacology. 31 (2023) 77-87. https://doi.org/10.1007/s10787-022-01092-x.

[61] M.M. Bashir, M.R. Sharma, V.P. Werth, TNF-α production in the skin, Archives of Dermatological Research. 301 (2009) 87-91. https://doi.org/10.1007/s00403-008-0893-7.

[62] F. Karadeniz, J.H. Oh, H.R. Kim, et al., Camellioside A, isolated from *Camellia japonica* flowers, attenuates UVA-induced production of MMP-1 in HaCaT keratinocytes via suppression of MAPK activation, Experimental and Therapeutic Medicine. 21 (2021) 16. https://doi.org/10.3892/etm.2020.9448.